Progress In Electromagnetics Research Letters, Vol. 5, 109–121, 2008

COMBINING PSEUDOSPECTRAL DISCRETIZATION WITH METHOD OF LINES IN FULL-WAVE ANALYSIS OF CYLINDRICAL MICROSTRIP

Z. H. Fan and R. S. Chen

Department of Communication Engineering
Nanjing University of Science and Technology
Nanjing 210094, China

Abstract—In this article, method of lines combined with pseudospectral discretization has been extended to the analysis of the characteristics of open cylindrical substrate microstrip lines. Numerical results show the combination benefits from the two methods which have higher efficiency and they are powerful alternative analytic tools.

1. INTRODUCTION

There are a lot of techniques in the modal analysis and dispersion analysis of transmission lines and waveguide structures [1–6]. The method of lines (MoL) [6–10] is a well-established numerical technique (or rather a semi-analytical method) for the analysis of transmission lines, waveguide structures, and scattering problem. The method was originally developed by mathematicians and used for boundary value problems in physics and mathematics. It was introduced into the EM community around 1980 and further developed by Pregla et al. and other researchers. The MoL in cylindrical coordinates (CMoL), which discretizes the Helmholtz in angular direction, is proposed by Xu [11] in 1988, and then there are a number of literatures about CMoL [12, 13]. MoL is regarded as a special finite difference method but more effective with respect to accuracy and computational time than the regular finite difference method. It basically involves discretizing a given differential equation in one or two dimensions while using analytical solution in the remaining direction. It does not yield spurious modes nor does it have the problem of "relative convergence" as in spectral method. Relative convergence is a well known phenomenon arising in the solution of truncated infinite sets of equations [19]. It is well known that the MoL provides only second-order accuracy. To break through this barrier in

the modern precious and fast analysis, a lot of high-order discretization methods of the Helmholtz equation have been developed [9]. Recently, pseudospectral disctretization [14], famous for its high accuracy and high convergence rate, has been introduced into MoL in the non-hybrid mode of the hollow metallic waveguide [15] and hybrid mode of the planar microstrip structure [16, 17].

Pseudospectral methods, which can be seen as high-accuracy limits of finite difference methods with special non-equally spaced grid distributions, provide a useful alternative to classic finite difference and finite element methods for the approximate solution of differential equations. Finite elements may sacrifice computational efficiency in exchange for great versatility at general boundaries. On the other extreme, spectral methods are often most effective in cases where the phenomenon under study occurs in the largely regular domains. Between them, pseudospectral methods are fortunately appropriate in a vast regime and can be adapted to most geometry arising in applications although less flexible than finite elements. Even when they employ high orders of approximation, the implementations for it still tend to be comparatively straightforward. In fact, pseudospectral method approximates functions and their derivatives by global arguments and with very smooth basis functions:

$$u(x) = \sum_{k=0}^{N} a_k \phi_k(x)$$

where the $\phi_k(x)$ are for example Chebyshev polynomials or trigonometric functions. This approach has notable strengths as follows: (1) For the analytic functions, the approximating error typically decays (as N increases) at exponential rather than at (much slower) polynomial rates. (2) The method is virtually free of both dissipative and dispersive errors. (3) The approach is surprisingly powerful for many cases in which both solutions and variable coefficients are non-smooth or even discontinuous. (4) Especially in several space dimensions, the relatively coarse grids that suffice for most accuracy requirements allow very time- and memory-efficient calculations. But for irregular domains and certain boundary conditions, it still has some difficulties and inefficiencies [14]. In this paper, pseudospectral method is introduced as a tool in the process of discretization in method of lines. Unlike conventional finite difference method, which approximates derivatives of a function with local arguments such as $du(x)/dx = [u(x+h) - u(x-h)]/2h$ and is typically designed to be exact for polynomials of low order, pseudospectral method is global, high order polynomial approximation.

Therefore, the solution accuracy for pseudospectral-based method of lines is highly improved [15–17]. Because only one dimension needs discretization for two-dimensional boundary values, the difficulties for pseudospectral method to treat irregular domain can also be partly avoided if it is combined with method of lines. The eigenvalues of hollow metallic waveguide and planar microstrip structure have been analyzed [15–17] and the pseudospectral MoL exhibits an excellent convergence speed. In this paper, it is exploited for the hybrid mode analysis of cylindrical microstrip lines and our results demonstrate that the pseudospectral MoL (PMoL) has much faster convergence speed than the conventional MoL in terms of the required number of lines.

2. THEORETICAL ANALYSIS

The principal steps in developing the MoL or PMoL algorithm are always the same, regardless the coordinate system. Therefore, the following mathematical steps are greatly abbreviated and we focus only on the aspects pertaining to the PMOL in cylindrical coordinates. Figure 1(a) shows the structure model of a cylindrical microstrip. A metal wall is placed at radius $R = r_1$, which is covered with a dielectric substrate. The dielectric substrate has a depth of $d = r_2 - r_1$ with dielectric constant ε_r. The width of the infinitely long microstrip line is denoted as $w = r_2\delta_\theta$, where δ_θ is the angular extent of the strip defined in the figure; the curvature coefficient, c, is introduced as the ratio

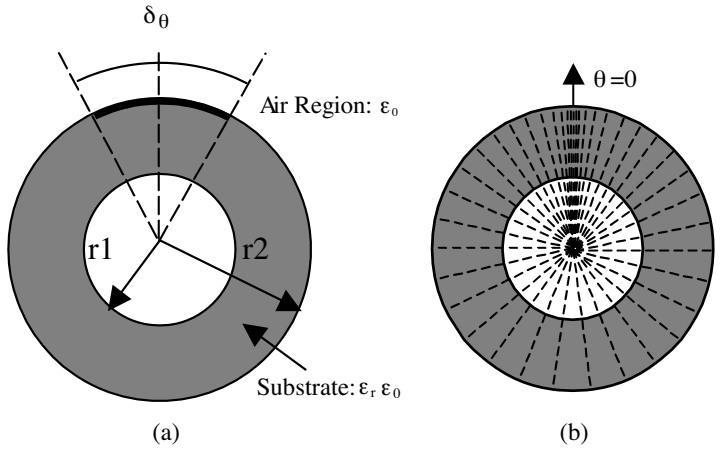

Figure 1. (a) The structure model of a cylindrical microstrip. (b) Pseudospectral discrete lines distribution by an example of total discrete lines $N = 40$.

of inner radius r_1 to outer radius r_2, namely, $c = r_1/r_2$. Figure 1(b) shows an example of PS discrete nodes distribution with the total lines $N = 40$, the nodes quadratically cluster near $\theta = 0$. It is obvious that with the same total lines, this one has more lines assigned metal strip than the MoL that uses equi-spaced discretizing. Under the cylindrical coordinate system, with the time harmonic dependence $\exp(j\omega t)$ being omitted for brevity, the field components E and H satisfy the following equations:

$$\begin{aligned} E_\theta &= \frac{1}{k^2-\beta^2}\left[-\frac{j\beta}{R}\frac{\partial E_z}{\partial \theta} + j\omega\mu\frac{\partial H_z}{\partial R}\right] \\ H_\theta &= \frac{1}{k^2-\beta^2}\left[-\frac{j\beta}{R}\frac{\partial H_z}{\partial \theta} - j\omega\varepsilon\frac{\partial E_z}{\partial R}\right] \end{aligned} \tag{1}$$

The z direction components E_z and H_z satisfy the Helmholtz equation:

$$\frac{1}{R}\frac{\partial}{\partial R}\left(R\frac{\partial \phi^{eh}}{\partial R}\right) + \frac{\partial^2 \phi^{eh}}{R^2\partial\theta^2} + \left(k^2-\beta^2\right)\phi^{eh} = 0 \tag{2}$$

where ϕ denotes E_z or H_z. Note that here ϕ can be expressed as

$$\phi = \phi^{eh}(R,\, \theta)\exp(-j\beta z)$$

where β is the phase constant.

Now the boundary conditions are needed to be properly selected. Thinking of the structure's symmetry, just half of the structure in Figure 1(a) is adopted to simplify the original problem. Here the periodical boundary condition is given up and Neumann-Dirichlet boundary (ND) for E_z and Dirichlet-Neumann boundary (DN) for H_z are adopted. In fact, when the microstrip operates with fundamental mode, this half structure can be truncated into a smaller one for the fact that the higher the frequency is, the more the electromagnetic wave's energy stays under the upper metal strip. From experience, when the truncated angular $\theta_N > (5-8)\delta_\theta$, the error in the high frequency analysis introduced by truncated is negligible.

For the given N, distinct nodes $0 = \theta_1 < \theta_2 < \ldots < \theta_{N-1} < \theta_N \leq 2\pi$ in the segment $[0, \theta_N]$ and the global method of differential quadrature, based on the high-order polynomial approximation, are first introduced. Following the idea of integral quadrature, it is assumed that any derivative at a grid point is approximated by a linear summation of all the functional values in the whole computational domain. For example, the first derivatives of $f(\theta)$ at a point θ_i are

approximated by

$$f'_{\theta}(\theta_i) = \sum_{j=1}^{N} b_{ij} f(\theta_j) \quad \text{for} \quad i = 1, 2, \ldots, N \tag{3}$$

where N is the number of grid points and b_{ij} are the weighting coefficients. To determine the weighting coefficients, b_{ij}, pseudospectral method assumes that $f(\theta)$ is approximated by a high-order polynomial,

$$f(\theta) = \sum_{k=1}^{N} c_k \theta^{k-1} \tag{4}$$

Then, under the analysis of a linear polynomial vector space, the following explicit formulation is used to compute b_{ij}:

$$b_{ij} = \frac{M^{(1)}(\theta_i)}{(\theta_i - \theta_j) M^{(1)}(\theta_j)} \quad \text{for} \quad j \neq i \tag{5a}$$

$$b_{ij} = -\sum_{j=1,\, j\neq i}^{N} b_{ij} \tag{5b}$$

where

$$M^{(1)}(\theta_k) = \prod_{j=1, j\neq k}^{N} (\theta_k - \theta_j) \tag{6}$$

In the above discussion, the sample points are arbitrary distribution in interval [0, θ_N]. In the pseudospectral method, each dependent variable in the differential problem is approximated by a polynomial of finite degree. The discrete approximating equations are then obtained by setting residuals to zero at an appropriate set of collocation points in the solution domain. The proper choice of collocation points is crucial in terms of accuracy, stability, and ease of implementation of boundary conditions. Usually, the equi-spaced node distribution is adopted but the large deviation is observed near the two endpoints in the pseudospectral method. The easiest way to offset these errors is to concentrate the nodes toward the ends of the interval. It is well known that the Chebyshev-distribution has smallest error and minimum node spacing, which decreases as $O(1/N^2)$. The Chebyshev-distribution characteristic of minimum node spacing enhances the ability to treat the irregular domain for discrete technique of pseudospectral method. For a given problem the pair

of boundary conditions are either Dirichlet-Neumann or Neumann-Dirichlet. The difference matrix with the *DN* lateral boundary condition is denoted by $[a_{DN}]$ and can be obtained as follows:

$$a_{i,j}^{DN} = b_{i+1,j+1} - b_{i+1,N+1}\frac{b_{N+1,j+1}}{b_{N+1,N+1}}$$
$$i = 1, 2, \ldots, N-1, \quad j = 1, 2, \ldots, N-1 \tag{7}$$

and the $[a_{ND}]$ for *ND* lateral boundary condition is as follows:

$$a_{i,j}^{ND} = b_{i+1,j+1} - b_{i+1,1}\frac{b_{1,j+1}}{b_{1,1}} \quad i = 1, 2, \ldots, N-1, \quad j = 1, 2, \ldots, N-1 \tag{8}$$

For the first derivative of E_z with respect to the θ-direction, one obtains

$$\frac{d\overline{E}_z}{d\theta} = [a_{ND}]\overline{E}_z \tag{9}$$

where $\overline{E}_z$ denotes the discretized E_z. Since E_z and H_z have dual boundary conditions, the finite difference expression for the first derivative of H_z becomes

$$\frac{d\overline{H}_z}{d\theta} = [a_{DN}]\overline{H}_z \tag{10}$$

Combining (9) and (10), one obtains for the second-order derivatives

$$\frac{d^2\overline{E}_z}{d\theta^2} = [a_{DN}]\frac{d\overline{E}_z}{d\theta} = [a_{DN}][a_{ND}]\overline{E}_z \tag{11}$$
$$\frac{d^2\overline{H}_z}{d\theta^2} = [a_{ND}]\frac{d\overline{H}_z}{d\theta} = [a_{ND}][a_{DN}]\overline{H}_z \tag{12}$$

For a homogeneous layer, the second order pseudospectral difference operators $D_{\theta\theta}^{e,h}$ are the products of two different first order operators and their eigenvalues $-\lambda_{e,h}^2$ and the eigenvector matrices $T^{e,h}$ are defined as follows:

$$\left[D_{\theta\theta}^{h}\right]\left[T^{h}\right] = [a_{ND}]\,[a_{DN}]\left[T^{h}\right] = \left[T^{h}\right]\left[\lambda_h^2\right] \tag{13}$$
$$[D_{\theta\theta}^{e}]\,[T^{e}] = [a_{DN}]\,[a_{ND}]\,[T^{e}] = [T^{e}]\left[\lambda_e^2\right] \tag{14}$$

where $\left[T^{e,h}\right]$ are eigenvector matrices of the second-order pseudospectral difference matrices. Although $D_{\theta\theta}^{e,h}$ are not symmetric, for these

real matrices there exist the real matrices $\left[T^{e,h}\right]$ such that

$$\left[T^{e,h}\right]^{-1}\left[D_{\theta\theta}^{e,h}\right]\left[T^{e,h}\right] = -diag\left[d_{\theta\theta n}^{2}\right] \tag{15a}$$

$$\begin{aligned}\left[T^{h}\right]^{-1}\left[a_{ND}\right]\left[T^{e}\right] &= diag\left[d_{\theta\theta n}\right]\\ \left[T^{e}\right]^{-1}\left[a_{DN}\right]\left[T^{h}\right] &= -diag\left[d_{\theta\theta n}\right]\end{aligned} \tag{15b}$$

where *diag* denotes a diagonal matrix; $\left[T^{h}\right]$ is directly solved from the Equation (13) and the $[T^{e}]$ is derived as follows [17]:

$$[T^{e}] = [a_{DN}]\left[T^{h}\right] diag\left[d_{\theta\theta n}^{-1}\right] \tag{16}$$

Along θ direction we perform a discretization by using N radial lines distributed as Chebyshev extreme nodes, as shown in Figure 1(b); it is:

$$\theta_k = \frac{\theta_N}{2}\left[1+\cos\frac{(k-1)\pi}{N-1}\right], \quad k = 1, 2, \ldots, N \tag{17}$$

where θ_N is truncated angular. Then differentials with respect to θ are taken place with differences; a set of coupled ordinary differential equations is obtained.

$$\frac{1}{R}\frac{\partial}{\partial R}\left(R\frac{\partial\Phi^{e,h}}{\partial R}\right) + \left(k^2-\beta^2-\left[D_{\theta\theta}^{e,h}\right]\right)\Phi^{e,h} = 0 \tag{18}$$

where $\Phi^{e,h}$ denote E_z or H_z; $\left[D_{\theta\theta}^{e,h}\right]$ are the second-order differential's discrete matrices of E_z or H_z; and the first-order differential's discrete matrices of E_z and H_z are $\left[D_{\theta}^{e,h}\right]$. A transformed potential vector $\overline{U}$ is now introduced,

$$\overline{U}^{\,e,h} = \left[T^{e,h}\right]^{-1}\Phi^{e,h} \tag{19}$$

then a set of decoupled ordinary equations with following forms can be got

$$\frac{1}{R}\frac{\partial}{\partial R}\left(R\frac{\partial\overline{U}_{\,i}^{\,e,h}}{\partial R}\right) + \left(k^2-\beta^2-\frac{d_{\theta\theta i}^{2}}{R^2}\right)\overline{U}_{\,i}^{\,e,h} = 0 \tag{20}$$

where $-d_{\theta\theta i}^{2}$ is the ith eigenvalue of the second-order matrix $\left[D_{\theta\theta}^{e,h}\right]$. The superscript e, h is eliminated since $d_{\theta\theta i}^{e,h}$ and $D_{\theta\theta}^{h}$ are the same in

PMOL. Where $\overline{U}_i^{e,h}$ is the ith element in the vector $\overline{U}^{e,h}$ and $\overline{U}^{e,h}$ is the transformation of the discrete z-direction components E_z or H_z.

Equation (20) is the one-dimensional Helmholtz equation corresponding to the Bessel functions, whose common resolutions can be written as:

$$\begin{aligned} U_i^{eh}(R) &= \begin{cases} A_{1i}^{eh} J_{\mu i}(Kc_1 R) + A_{2i}^{eh} N_{\mu i}(Kc_1 R) & r_1 < R < r_2 \\ A_{3i}^{eh} K_{\mu i}(Kc_2 R) & R > r_2 \end{cases} \\ Kc_1 &= \sqrt{K_1^2 - \beta^2} \quad Kc_2 = \sqrt{\beta^2 - K_2^2} \end{aligned} \tag{21}$$

where $\mu i = d_{\theta\theta i}$ and A_{1i}^{eh}, A_{2i}^{eh}, A_{3i}^{eh} are coefficients to be determined; J, N, K are Bessel, Neumann, and modified Bessel functions, respectively. In region 2, we omit the first modified Bessel function I because it does not satisfy the fields boundary conditions in the infinity.

Now we give the details of the derivation of the Green's admittance matrix in the transformation domain. For tangential fields at $R = r_1$, i.e.,

$$\overline{E}_z\big|_{R=r_1} = 0 \quad \left.\frac{\partial \overline{H}_z}{\partial R}\right|_{R=r_1} = 0$$

$$\begin{aligned} \overline{E}_{zi} &= \begin{cases} B^e \left[G J_{\mu i}(Kc_1 R) + N_{\mu i}(Kc_1 R) \right] \\ C^e \left[K_{\mu i}(Kc_2 R) \right] \end{cases} \\ \overline{H}_{zi} &= \begin{cases} B^h \left[D J_{\mu i}(Kc_1 R) + N_{\mu i}(Kc_1 R) \right] \\ C^h \left[K_{\mu i}(Kc_2 R) \right] \end{cases} \end{aligned} \tag{22}$$

the "$-$" above the vector denotes in the transformation domain. Where

$$G = -\frac{N_{\mu i}(Kc_1 r_1)}{J_{\mu i}(Kc_1 r_1)} \quad D = -\frac{N'_{\mu i}(Kc_1 r_1)}{J'_{\mu i}(Kc_1 r_1)}$$

then at $R = r_2$

$$\begin{aligned} \left.\frac{\partial \overline{E}_{z1}}{\partial R}\right|_{R=r_2} &= \frac{Kc_1 \left[G J'_{\mu i}(Kc_1 r_2) + N'_{\mu i}(Kc_1 r_2) \right]}{G J_{\mu i}(Kc_1 r_2) + N_{\mu i}(Kc_1 r_2)} \overline{E}_{z1} = P \overline{E}_{z1} \\ \left.\frac{\partial \overline{H}_{z1}}{\partial R}\right|_{R=r_2} &= \frac{Kc_1 \left[D J'_{\mu i}(Kc_1 r_2) + N'_{\mu i}(Kc_1 r_2) \right]}{D J_{\mu i}(Kc_1 r_2) + N_{\mu i}(Kc_1 r_2)} \overline{H}_{z1} = Q \overline{H}_{z1} \end{aligned} \tag{23a}$$

and

$$\begin{aligned} \left.\frac{\partial \overline{E}_{z2}}{\partial R}\right|_{R=r_2} &= \frac{Kc_2 K'_{\mu i}(Kc_2 r_2)}{K_{\mu i}(Kc_2 r_2)}\overline{E}_{z2} = T\overline{E}_{z2} \\ \left.\frac{\partial \overline{H}_{z2}}{\partial R}\right|_{R=r_2} &= T\overline{H}_{z2} \end{aligned} \tag{23b}$$

with the transformation

$$\begin{aligned} \overline{E}_\theta &= \left[T^h\right]^{-1} E_\theta \qquad \overline{H}_\theta = [T^e]^{-1} H_\theta \\ \overline{J}_\theta &= [T^e]^{-1} J_\theta \qquad \overline{J}_z = \left[T^h\right]^{-1} J_z \end{aligned} \tag{24}$$

continuity boundary at $R = r_2$ is

$$\begin{aligned} \overline{E}_{z1} &= \overline{E}_{z2} \qquad \left(\overline{H}_{z1} - \overline{H}_{z2}\right) = -\overline{J}_\theta \\ \overline{E}_{\theta 1} &= \overline{E}_{\theta 2} \qquad \overline{H}_{\theta 1} - \overline{H}_{\theta 2} = \overline{J}z \end{aligned} \tag{25}$$

From (1), we can get

$$\begin{cases} \overline{E}_{\theta 1} = \dfrac{1}{Kc_1^2}\left[-\dfrac{j\beta}{R_2}\xi\overline{E}_{z1} + j\omega\mu Q\overline{H}_{z1}\right] \\ \overline{H}_{\theta 1} = \dfrac{1}{Kc_1^2}\left[\dfrac{j\beta}{R_2}\xi\overline{H}_{z1} - j\omega\varepsilon_1 P\overline{E}_{z1}\right] \end{cases} \tag{26a}$$

$$\begin{cases} \overline{E}_{\theta 2} = -\dfrac{1}{Kc_2^2}\left[-\dfrac{j\beta}{R_2}\xi\overline{E}_{z2} + j\omega\mu T\overline{H}_{z2}\right] \\ \overline{H}_{\theta 2} = -\dfrac{1}{Kc_2^2}\left[\dfrac{j\beta}{R_2}\xi\overline{H}_{z2} - j\omega\varepsilon T\overline{E}_{z2}\right] \end{cases} \tag{26b}$$

where $\xi = \mu_i$, after some operations, we can get the following equation:

$$\begin{bmatrix} \overline{J}_{\theta i} \\ \overline{J}_{zi} \end{bmatrix} = \begin{bmatrix} G_{11} & G_{12} \\ G_{21} & G_{22} \end{bmatrix} \begin{bmatrix} \overline{E}_{\theta i} \\ \overline{E}_{zi} \end{bmatrix} \tag{27}$$

where

$$G_{11} = \frac{1}{j\omega\mu}\left[\frac{Kc_1^2}{Q} + \frac{Kc_2^2}{T}\right] \quad G_{12} = \frac{\beta}{\omega\mu r_2}\xi\left[\frac{1}{Q} - \frac{1}{T}\right]$$

$$G_{21} = G_{12} \quad G_{22} = \frac{-\beta^2\xi^2}{r_2^2 j\omega\mu}\left(\frac{1}{Kc_1^2 Q} + \frac{1}{Kc_2^2 T}\right) - \left(\frac{\varepsilon_r P}{Kc_1^2} + \frac{T}{Kc_1^2}\right) j\omega\varepsilon_0$$

Q and T are defined in equation (23). So we can find

$$\begin{bmatrix} \overline{E}_{\theta i} \\ \overline{E}_{zi} \end{bmatrix} = \left[\overline{Z} \right] \begin{bmatrix} \overline{J}_{\theta i} \\ \overline{J}_{zi} \end{bmatrix} \tag{28}$$

After transforming back to the spatial domain and taking into account that the tangential electric field vanishes on the metallic strip, a reduced matrix equation is obtained:

$$[Z]_{red} \begin{bmatrix} J_{\theta i} \\ J_{zi} \end{bmatrix}_{red} = \begin{bmatrix} E_{\theta i} \\ E_{zi} \end{bmatrix}_{red} = 0 \tag{29}$$

The propagation constants or effective dielectric constant can be found form the corresponding determinantal equation:

$$DET\,|Z(\beta)|_{red} = 0 \tag{30}$$

It is a real equation to find a real root.

3. NUMERICAL RESULTS

The effective dielectric constants for several structures are computed by using MoL and PMoL respectively. Figure 2 reveals how the curved surface affects the effective dielectric constant; the parameters are

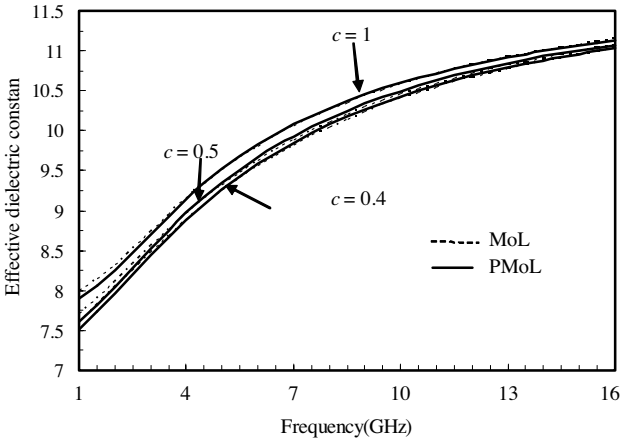

Figure 2. The effective dielectric constant results versus the operation frequency of a cylindrical microstrip with different curvature coefficient using MoL and PMoL. The parameters are $\varepsilon_r = 11.7$, d= 0.317 cm and $w/d = 1$.

$\varepsilon_r = 11.7$, $d = 0.317\,\text{cm}$ and $w/d = 1$. The analysis region is limited in $0 < \theta < 5\delta_\theta$ and total line number N along θ direction is 35 in MoL and 15 in PMoL.

Note that the difference for effective dielectric constant at low frequencies between the two methods is a little bigger; but from reference [18], we can find that these data are all in the error ranges.

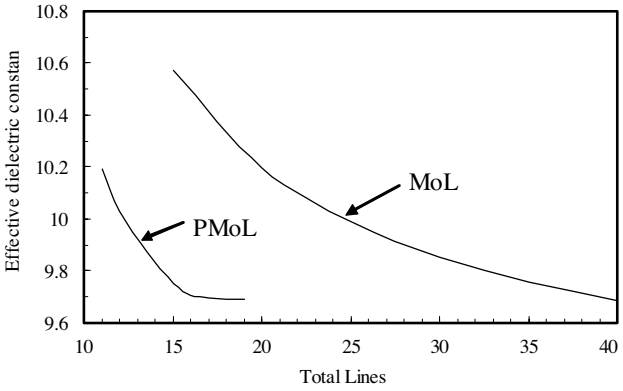

Figure 3. Convergence of the PMoL and MoL with frequency 6.5 GHz and $c = 0.5$.

The convergence curves are given in Figure 3. The operation frequency is 6.5 GHz; the structure parameter is the same as shown in Figure 1(a); and $c = 0.5$. It can be found that the pseudospectral MoL has much faster convergence rate than the conventional MoL. The new developed pseudospectral MoL adopts high-order interpolation polynomial to approximate the derivatives in controlling equation. As a result, it can approximate the smooth field inside the domain of interest so that the solution not only is analytical along line direction but also maintains high accuracy in discrete direction. Although the second-order differential matrix for the pseudospectral MoL is not sparse as that in conventional second-order MoL, the eigenvalues, eigenvectors and transformation matrix can be numerically solved by matured algorithm and the computation cost is little because of fewer lines needed in the numerical simulation.

4. CONCLUSIONS

In this paper, the novel pseudospectral MoL to solve time-harmonic electromagnetic problem is introduced and the basic concept and theory are described in details through the hybrid mode analysis of cylindrical microstrip lines. Some numerical results are given to

demonstrate the efficiency and accuracy of this method. It can be seen that the pseudospectral MoL has a much faster convergence speed and it can achieve high accuracy in both analytical and discretized direction.

REFERENCES

1. Chang, H.-W. and M.-H. Sheng, "Field analysis of dielectric waveguide devices based on coupled transverse-mode integral equation — mathematical and numerical formulations," *Progress In Electromagnetics Research*, PIER 78, 329–347, 2008.
2. Singh, V., Y. K. Prajapati, and J. P. Saini, "Modal analysis and dispersion curves of a new unconventional bragg waveguide using a very simple method," *Progress In Electromagnetics Research*, PIER 64, 191–204, 2006.
3. Hernandez-Lopez, M. A. and M. Quintillan-Gonzalez, "A finite element method code to analyse waveguide dispersion," *J. of Electromagn. Waves and Appl.*, Vol. 21, No. 3, 397–408, 2007.
4. Zhou, X. and G. W. Pan, "Application of physical spline finite element method (PSFEM) to fullwave analysis of waveguides," *Progress In Electromagnetics Research*, PIER 60, 19–41, 2006.
5. Tang, M. and J. F. Mao, "Transient analysis of lossy nonuniform transmission lines using a time-step integration method," *Progress In Electromagnetics Research*, PIER 69, 257–266, 2007.
6. Pregla, R. and W. Pascher, "The method of lines," *Numerical Techniques for Microwave and Millimeter-wave Passive Structures*, T. Itoh (ed.), 381–446, Wiley, New York, 1989.
7. Chen, R. S. and D. G. Fang, "Analysis of the open microstrip lines by method of lines," *International Journal of Microwave and Millimeter Wave CAD Engineering*. Vol. 3, No. 2, 109–113, 1993.
8. Preglas, R., "MOL-BPM method of lines based beam propagation method," *Progress In Electromagnetics Research*, PIER 11, 51–102, 1995.
9. Pregla, R., "Higher order approximation for the difference operators in the method of lines," *IEEE Microwave and Guided Wave Lett.*, Vol. 5, No. 2, 53–55, Feb. 1995.
10. Helfert, S. F., "Applying oblique coordinates in the method of lines," *Progress In Electromagnetics Research*, PIER 61, 271–278, 2006.
11. Xu, Y., "Application of the method of lines to solve problems

in cylindrical coordinates," *Microwave and Optical Technology Letters*, Vol. 1, No. 5, 173–175, July 1988.

12. Chen, R. S., D. G. Fang, and X. G. Li, "Analysis of open microstrip lines by MOL," *International Journal of Microwave and Millimeter-wave Computer-aided Engineering*, Vol. 3, No. 2, 109–113, 1993
13. Xiao, S., et al., "Analysis of cylindrical transmission lines with the method of lines," *IEEE Trans. Microwave Theory Tech.*, Vol. 44, No. 7, 993–999, July 1996.
14. Fornberg, B., *A Practical Guide to Pseudospectral Methods*, Cambridge University Press, 1996.
15. Chen, R. S., E. K. N. Yung, K. Wu, and Y. F. Han, "The generalized method of lines based on discretisation technique of pseudospectral method," *Microwave and Optical Technology Letters*, Vol. 20, No. 5, 249–254, 1999.
16. Chen, R. S., D. X. Wang, and E. K. N. Yung, K. Wu, "Analysis of three-dimensional MMIC by spectral-pseudospectral domain technique," *Microwave and Optical Technology Letters*, Vol. 31, No. 5, Dec. 5, 2001.
17. Chen, R. S., Z. H. Fan, E. K. N. Yung, and C. H. Chan, "Hybrid mode analysis of microstrip lines by the method of lines with pseudospectral discretization," *Microwave and Optical Technology Letters*, Vol. 35, No. 3, 224–227, 2002.
18. Sarkar, T., "Finite difference frequency-domain treatment of open transmission structures," *IEEE Trans. Microwave Theory Tech.*, Vol. 38, 1609–1616, 1990.
19. Hofmann, H., "Relative convergence in mode-matching solutions of microstrip problems," *Electronics LettersL*, Vol. 10 No. 8, 126–127, 1974.